URTeC: 257

Assessing The Stratigraphic Variations In Geomechanical Properties Of The United Kingdom Bowland Shale Using Wireline And Seismic Data: How Could These Guide The Placement Of Lateral Wells?

Iain Anderson*[1], Jingsheng Ma[1], Xiaoyang Wu[2], Dorrik Stow[1], John R. Underhill[1], 1. Heriot-Watt University, 2. British Geological Survey.

Abstract

This work forms part of a study addressing the multi-scale heterogeneous and anisotropic rock properties of the Lower Carboniferous (Mississippian) Bowland Shale; the UK's most prospective shale-gas play. The specific focus of this work is to determine the geomechanical variability within the Preese Hall exploration well and, following a consideration of structural features in the basin, to consider the optimal position of productive zones for hydraulic fracturing. Positioning long-reach horizontal wells is key to the economic extraction of gas, but their placement requires an accurate understanding of the local geology, stress regime and structure. This is of importance in the case of the Bowland Shale because of several syn- and post-depositional tectonic events that have resulted in multi-scale and anisotropic variations in rock properties. Seismic, Well and Core data from the UK's first dedicated shale-gas exploration programme in NW England have all been utilized for this study. Our workflow involves; (1) summarizing the structural elements of the Bowland Basin and framing the challenges these may pose to shale-gas drilling; (2) making mineralogical and textural-based observations using cores and wireline logs to generate mineralogy logs and then to calculate a mineral-based brittleness index along the well; (3) developing a geomechanical model using slowness logs to determine the breakdown stress along the well; (4) placing horizontal wells guided by the mineral-based brittleness index and breakdown stress. Our interpretations demonstrate that the study area is affected by the buried extension of the Ribblesdale Fold Belt that causes structural complexity that may restrict whether long-reaching horizontal wells can be confidently drilled. However, given the thickness of the Bowland Shale, a strategy of drilled multiple, stacked laterals has been proposed. The mineralogical and geomechanical modelling presented herein suggests that several sites retain favorable properties for hydraulic fracturing. Two landing zones within the Upper Bowland Shale alone are suggested based on this work, but further investigation is required to assess the impact of small-scale elastic property variations in the shale to assess potential for well interference and optimizing well placement.

Introduction

The Lower Carboniferous (Mississippian) Bowland Shale is considered the most prospective shale play in the UK. Exploration has focused thus far in the Bowland Basin of Lancashire; where five dedicated shale-gas exploration wells have been drilled and one 3D seismic survey acquired. The wells include two

horizontal sections, one of which has produced encouraging initial flow test results (Cuadrilla Resources, 2019). In contrast to successful US plays, however, the Bowland Shale has experienced a complex series of tectonic events during, and since burial. These give rise to geological challenges at multiple scales that need consideration when assessing a shale-gas play. Geological and structural heterogeneity as observed using core, micro-imagery and logging data will have an impact on geomechanical properties and thus the formation's response to hydraulic fracturing. At a larger scale, the layer anisotropy and faulting will likely influence its geophysical behaviour and impact seismic processing, interpretation and attribute inversion. Finally, the structural complexity inherited from its tectonic history may restrict the scope to drill long-reaching horizontal wells necessary to produce gas at economic rates.

In this work, the structural history of the basin is briefly summarized in the context of drilling long-reaching lateral wells. The concept of targeting the Bowland Shale using multiple, stacked lateral wells is proposed, before a presenting an analysis of the geomechanical properties through the shale, to select zones where potential lateral wells could be placed.

Regional Structure

The Early Carboniferous structural framework of North England consists of a series of blocks and basins (Figure 1(a)) formed during Late Paleozoic intracontinental rifting on the northern margin of the Rheic Ocean. Basin strike varies from SW-NE to NW-SE in response to reactivation of the underlying Caledonian (Iapetus and Tornquist) lineaments (Corfield et al., 1996; Fraser and Gawthorpe, 2003) and is also influenced by the presence of Caledonian granites (Bott, 1967; Johnson, 1967). All the basins created effectively delineate prospective shale-gas basins such as the Bowland Basin, Cleveland Basin, Widmerpool Gulf and Gainsborough Trough. The region was tectonically active throughout the Carboniferous period and the subsequent closure of the Rheic Ocean and the Variscan Orogeny in the Late Carboniferous-Early Permian resulted in the development of a major fold-and-thrust systems in Northern Europe and Southern England. Although they lay to the north of the "Variscan thrust front", foreland areas of northern Britain felt the far-field stresses (Corfield et al., 1996). In the Bowland region, this was reflected in the fault reactivation (structural inversion) of pre-existing SW-NE striking extensional faults to create a zone of transpression known as the Ribblesdale Fold Belt (Arthurton, 1984) and significant erosion of Carboniferous sediments (Fraser and Gawthorpe, 2003). The area subsequently formed the eastern fringe of the East Irish Sea Basin, a major depocentre that formed in Permo-Triassic times, subsided through the Mesozoic and was subject to major uplift and exhumation during the Cenozoic.

Bowland Basin Structure

The Bowland Basin, which forms the focus of this work, is located in the north-west of England, between the Pennine Hills and the Lancashire coast (Figure 1(c)). It is the target of the first dedicated shale-gas exploration program in the UK but presents several geological challenges to successful drilling/production. Firstly, it sits buried beneath a Permo-Triassic cover in proximity; along-strike and down-plunge from a complex series of NE-SW trending anticlines that collectively make up the Ribblesdale Fold Belt. These features formed initially through syn-depositional extensional activity throughout Early Carboniferous times (Arthurton, 1984), but later reactivated during Variscan compression (Kirby et al., 2000). Should this style of deformation persist beneath the Base-Permian Unconformity into the Bowland Basin, it would be expected to see some evidence of

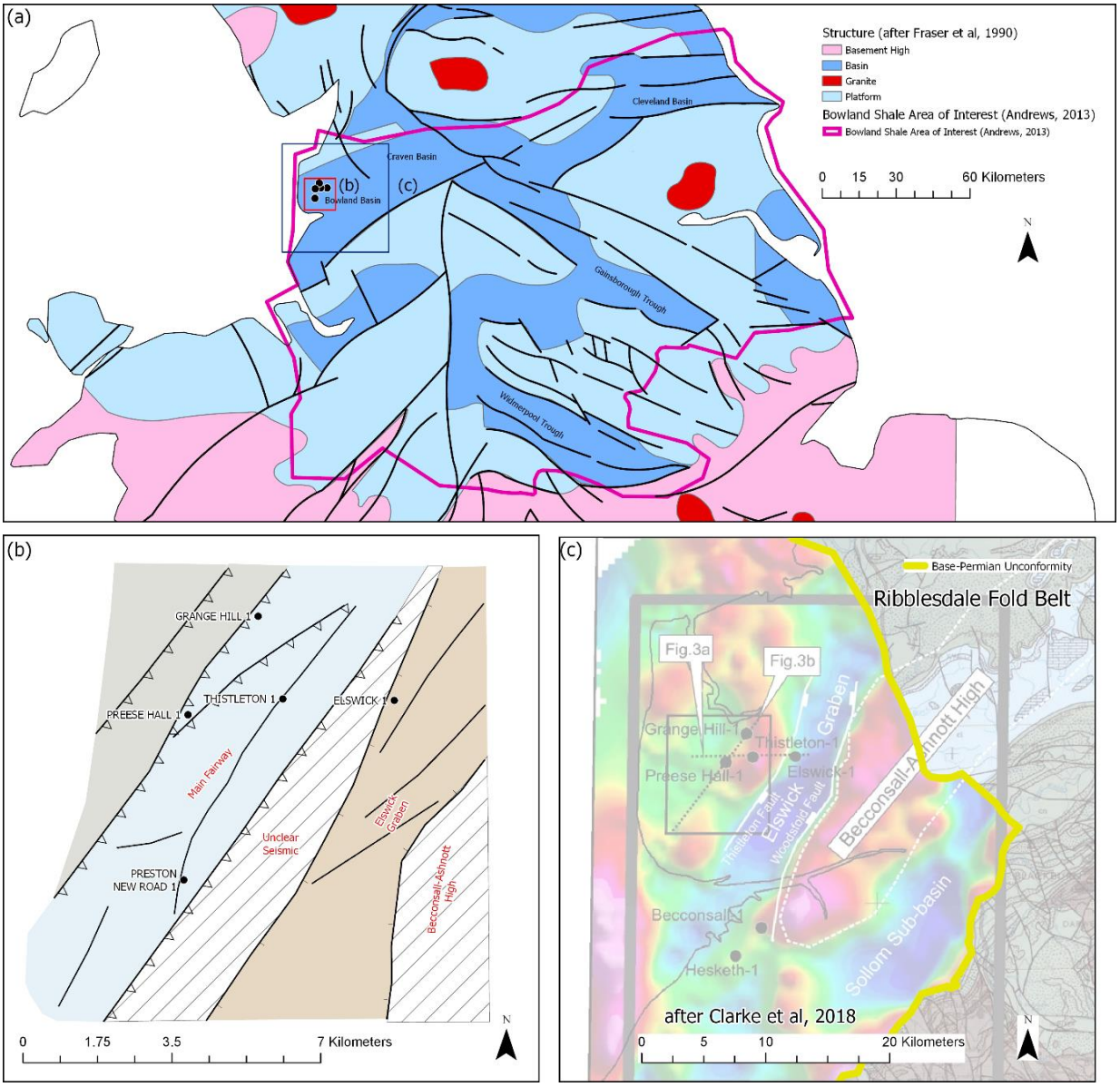

Figure 1 (a) Early Carboniferous structural elements of North England and Wales (reproduced after Fraser et al (1990). The prospective shale-gas region identified by the British Geological Survey is outlined in pink, and key basins are labelled. The region can be summarised as a series of blocks and basins, with mudstone-dominated sequences filling the basins, and carbonate sequences developing on the blocks. (b) Simplified structural elements map for the Bowland Basin produced at Lower Bowland Shale level using 3D seismic data. A NE-SW structural trend dominates with several SW-dipping reverse faults present. (c) Combination gravity and surface geology map of the Flyde region

wrench faulting and folding on seismic data, which could further compartmentalize the zones for drilling. Clarke et al (2018) presented a gravimetric map illustrating that the NE-SW structural trend in the Ribblesdale region continued into the Bowland Basin (Figure 1(c)). Our initial fault mapping using 3D seismic data confirms this (Figures 1(b) and 2) but requires further work. Such deformation may restrict an Operator's ability to drill long-reaching horizontal wells in the region. The concept of production using stacked, multi-lateral horizontal wells in this basin has been briefly proposed in the literature (Clarke et al., 2018, 2014a) but there has not been a systematic study of the geomechanical properties of the Bowland Shale with the view to identify where such laterals may be placed. This work seeks to assess the geomechanical properties of the Preese Hall well, using standard transformations of wireline log data calibrated to test data where possible. Furthermore, the properties are ranked using cluster analysis to systematically identify the most favorable regions.

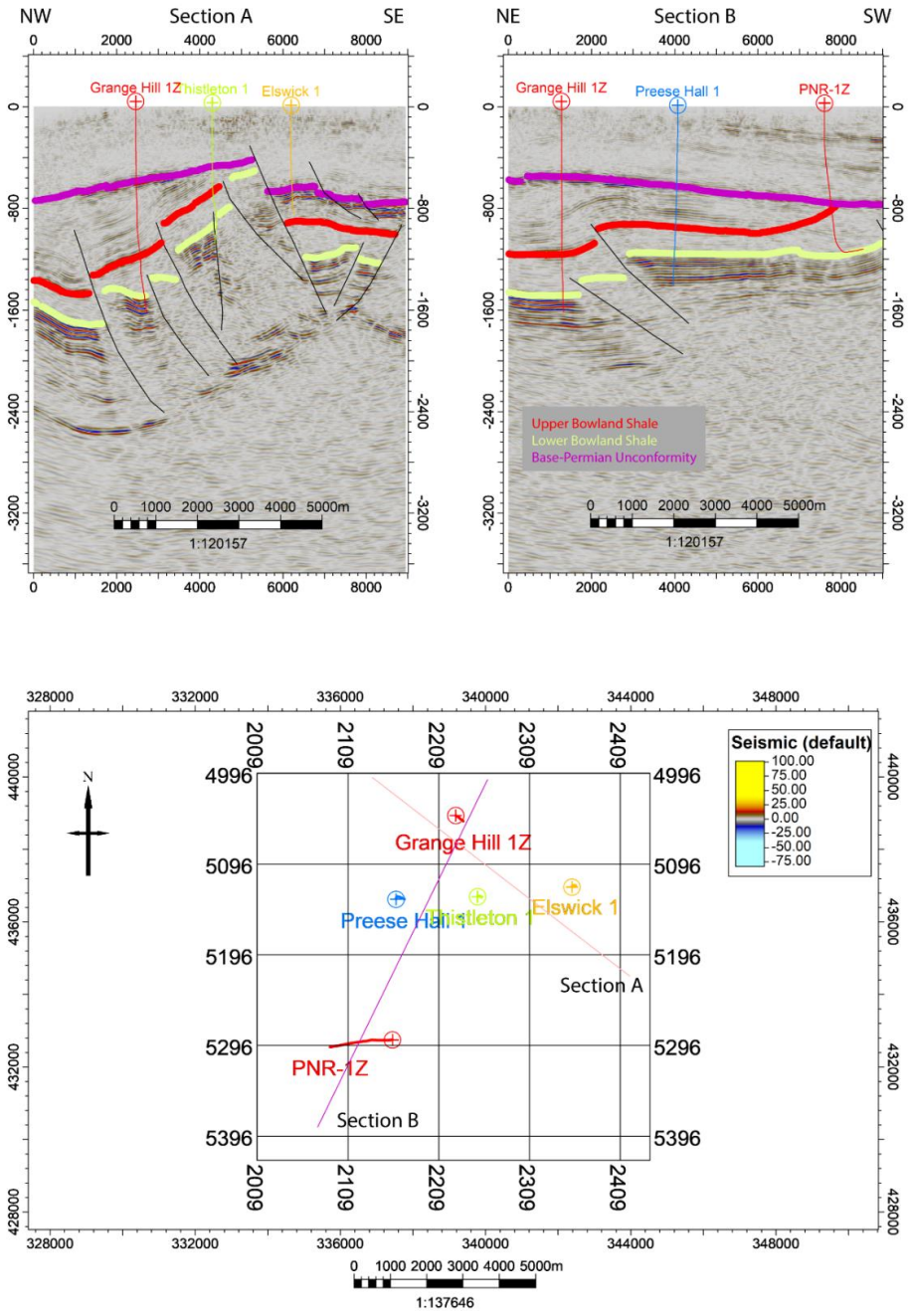

Figure 2: Example seismic cross-sections illustrating the structural style within the Bowland Basin. Section A illustrates a composite section approximately perpendicular to main structural trend. Section B illustrates a composite line along the main fault block. The region is intensely structured with a number of SW-dipping reverse faults. The thickness of the Upper Bowland Shale and the overlying Millstone Grit is shown to vary considerably across the survey, with evidence of erosion to the east of the Thistleton 1 well (see Section A) and further south at the PNR-1Z well.

The Preese Hall borehole

Cuadrilla Resources' Preese Hall well was drilled in 2010 and was the UK's first shale-gas exploration well. It encountered the Upper Bowland Shale at 1980m TVD, and the Lower Bowland Shale at 2475m. The interval was fully logged by wireline, including specialized tools such as cross-dipole sonic (CXD) and formation micro-imagery (FMI) which are publicly available, and accessed for this study. The Bowland Shale was divided into an Upper and Lower unit by the Operator at the Visean-Namurian

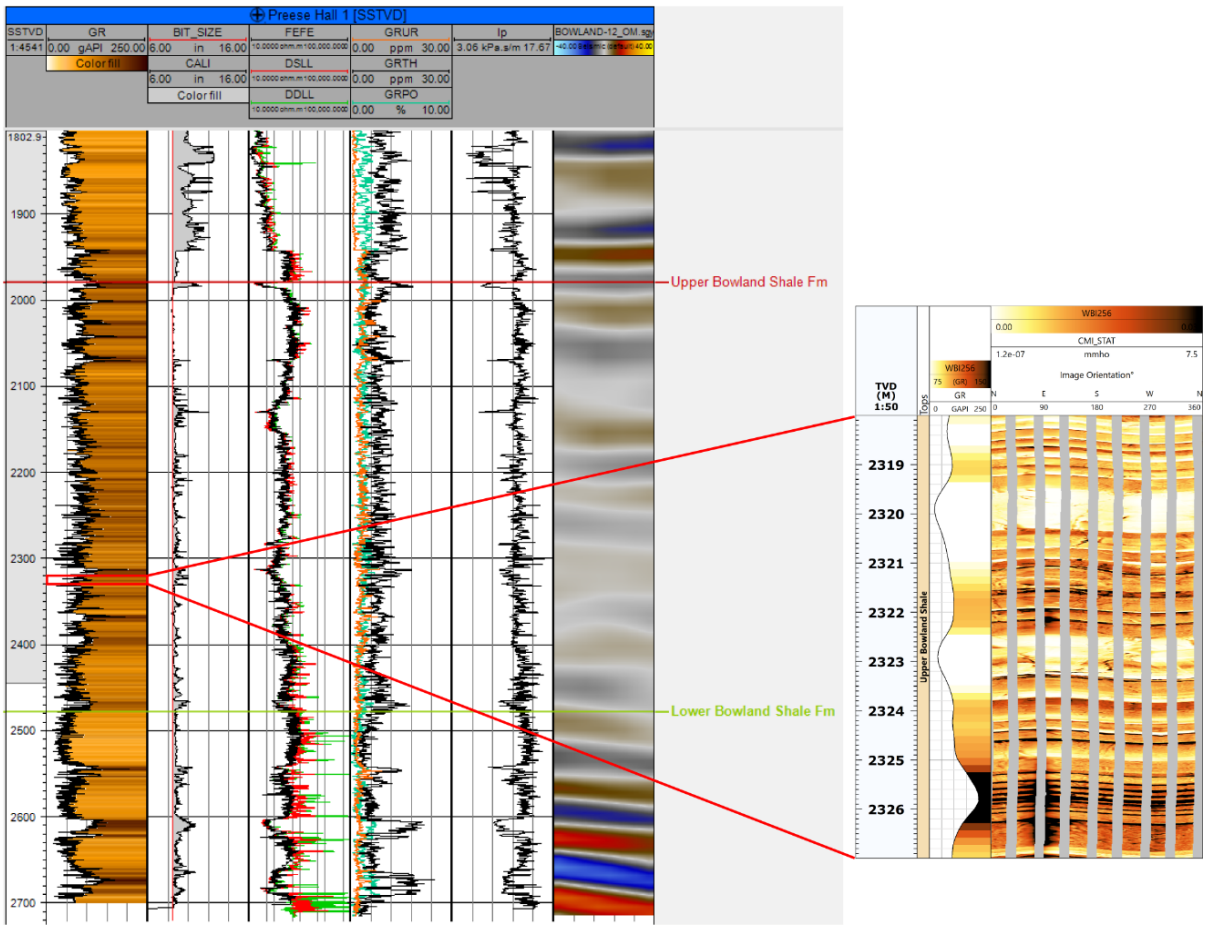

Figure 3: Wireline logs, well-seismic and FMI log for the Preese Hall well. The two sub-units of the Bowland Shale show contrasting characters both on logs and seismic. At the 10s cm scale, there is evidence of layering which is not captured at "traditional" wireline log resolution

boundary (Earp et al., 1961) following biostratigraphy analysis on core samples (Clarke et al., 2018). The two sub-units have marked differences in log and seismic character (Figure 3). The Lower Bowland Shale consists of alternating shales and calcareous sandstones which are sufficiently thick to be visualized on seismic. The Upper Bowland Shale consists of a heterogeneous package of thinner mudstones, carbonates and siltstones. These units are generally smaller than seismic resolution and thus poorly resolved. These differences are likely related to the transition syn-rift to post-rift deposition at the Visean-Namurian boundary (Fraser and Gawthorpe, 2003).

The heterogeneity evident from the wireline logs could pose another geological challenge to shale-gas production. In addition to the active tectonism discussed previously, the shale was influenced by nearby large carbonate (i.e. adjacent platforms) and clastic (i.e. the Pendle delta to the north) systems (Waters et al., 2009). At log-scale, this heterogeneity is expressed as the presence of low Gamma Ray calcareous and siliceous turbidites possibly transported into the basin during storm events. From observing the FMI log, layering at the 10s cm scale can be seen. Assuming the elastic properties of these layers are contrasting, this could pose problems for hydraulic fracture propagation. A transition from low to high minimum stress, or high to low brittleness will all restrict a fracture's ability to propagate across that boundary (Economides and Martin, 2007).

Methods

Mineralogy model

A continuous mineralogy is first determined using Schlumberger's ELAN solver. The method inverts volumetric fractions of a user-defined set of minerals and fluids using a combination of well logs and response equations. For this study; bulk density, neutron-porosity, deep resistivity, compressional sonic, thorium and potassium gamma were chosen as inputs. Clay, quartz, carbonate, pyrite and kerogen were selected as outputs. Default model parameters were chosen with the exception of mineral end-points, which were adjusted to provide a reasonable fit to XRD measurements.

Brittleness Index

Brittleness Index (BI) is a key parameter in evaluating a shale-gas reservoir and determining its geomechanical behaviour. Because of its widespread use, a vast number of definitions have been proposed by researchers; most of which were summarized in Zhang et al (2016)'s work. When considering wireline-log data, most of these methods are computed either from a mineralogical log (e.g. Jarvie et al (2007)), CXD log (e.g. Rickman et al (2008)) or through using empirical relationships (e.g. Jin et al (2014)). A mineralogy-based BI is used for this study, whereby quartz, carbonate and pyrite are considered brittle minerals (Zhang et al., 2017):

$$BI = \frac{W_{quartz} + W_{carbonate} + W_{pyrite}}{W_{total}}$$

Vertical Stress

As part of the geomechanical model, three principal stresses; vertical stress (σ_v), minimum horizontal stress (σ_h) and maximum horizontal stress (σ_H) need to be determined (Peng and Zhang, 2007). The vertical (or overburden) stress at a depth is considered as the weight imposed by the overlying formations. This is calculated through integration of the bulk density log and gravitational constant from the surface to the depth, denoted as z as follows (Jaeger et al., 2007):

$$\sigma_v = \int_0^z \rho\,(z) g dz$$

The calculation was extrapolated up to shallow zones without density log data (<600m) using a geometric fit tied to the mud line density.

Pore Pressure

In order to determine σ_h and σ_H parameters, which are to be back calculated from effective horizontal stresses, the pore pressure gradient (P_{pg}) needs to be estimated. Several methods have been proposed for predicting pore pressure using petrophysical logs, and when the appropriate model is chosen and calibrated to real data, accurate results can usually be achieved (Zhang, 2011). One of the most popular methods is the Eaton (1975) technique; an empirically-derived formula describing the difference between normal shale log response and overpressured shale log response and calibrated using the Eaton exponent. For this study, the sonic derivation is used as:

$$P_{pg} = OBG - (OBG - P_{ng})\left(\frac{\Delta t_n}{\Delta t}\right)^{\alpha}$$

Where OBG is the overburden stress gradient, P_{ng} is the hydrostatic pore pressure gradient and Δt is the Sonic transit time obtained from the well log. The two main parameters that need determined and could impose uncertainty are the normally-pressurized shale transit time Δt_n and the Eaton exponent, α. Selecting a Δt_n value can be challenging, and is usually determined through fitting a trendline to the sonic data in normally-pressured shale intervals. Using this method, a gradient of 7.8 µs/ft per km was calculated. The α parameter is then fitted using Diagnostic Fracture Injection Testing (DFIT) calibration data presented in Clarke et al (2018).

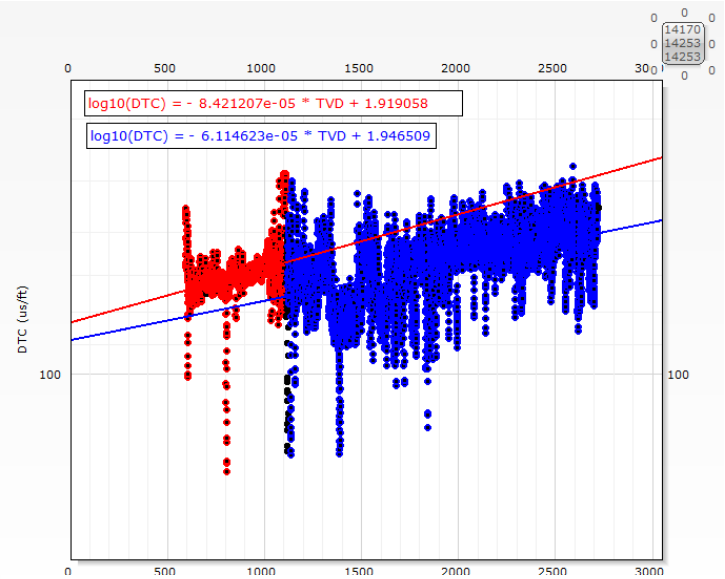

Figure 4: Sonic travel time versus true vertical depth for the Carboniferous and Permian formations in Preese Hall. The red data-points correspond to Permian post-Variscan formations, whereas the blue correspond to Carboniferous pre-Variscan formations. The two contrasting trendlines will impact pore pressure modelling.

A key pitfall of the Eaton method is the assumption that Δt_n will increase uniformly down the wellbore, and that if determined within a normally-pressured interval, it can then be extrapolated further down the section If the formations have undergone multiple periods of uplift and burial, multiple compaction trends would be expected, thus restricting the Eaton approach. As an example, slowness is plotted versus TVD in Figure 4 to illustrate the two different compaction trendlines (least squares regression) above (red) and below (blue) the Variscan unconformity (red). Once the trendline was selected, the Eaton exponent, α was reduced to 2 to provide a reasonable fit to the DFIT data.

Horizontal Stresses

The poroelastic-strain equation is one of the most commonly used methods for predicting σ_v and σ_H at depth using wireline logging data. The formula combines Terzaghi's effective stress theory with a third tectonic term (Prats, 1981):

$$\sigma_{\mathrm{h}} = \frac{\nu}{1-\nu}(\sigma_v - \alpha\sigma_{\mathrm{p}}) + \alpha\sigma_{\mathrm{p}} + \frac{E}{1-\nu^2}\varepsilon_h + \frac{\nu E}{1-\nu^2}\varepsilon_H$$

$$\sigma_{\mathrm{H}} = \frac{\nu}{1-\nu}(\sigma_v - \alpha\sigma_{\mathrm{p}}) + \alpha\sigma_{\mathrm{p}} + \frac{E}{1-\nu^2}\varepsilon_H + \frac{\nu E}{1-\nu^2}\varepsilon_h$$

Where σ_p is the pore pressure by integrating the pore pressure gradient (P_{ng}) determined using the Eaton method outlined above, α is the Biot's coefficient, E is static Young's modulus and ν is static Poisson's ratio. The static E and ν inputs were calculated by first obtaining a static/dynamic relationship from core samples in a nearby well, and then applying this transformation to CXD log data. Using these methods, E was calculated to be between of 15 and 30 GPa, and ν between 0.1 and 0.2. ε_h and ε_H are tectonic strain parameters that require fitting to calibration data. For this work, a α of 1 is used, ε_h is chosen as 1e-4 and ε_H is chosen as 1e-3 based on calibration to the DFIT and break-out data presented in Clarke et al (2018).

Formation Breakdown Pressure

Once the in-situ stresses are determined, they are combined with tensile rock strength (T_0) to calculate the formation breakdown pressure (P_b); a pressure that needs to be overcome in order to initiate a new

fracture in the formation. This is achieved when the effective stress becomes equal to the negative tensile strength of the rock, $-T_0$. (Economides and Nolte, 2000). T_0 was calculated as (Zoback, 2007):

$$UCS = 0.0528E^{0.712}; T_0 = \frac{UCS}{10}$$

Where UCS is the uniaxial compressive strength and E is the static Young's modulus. T0 was calculated to range between 6 and 9 MPa. P_b is then calculated as (Hubbert and Willis, 1957):

$$P_b = 3\sigma_h - \sigma_H - \sigma_p + T_0$$

Cluster Analysis

In order to define landings for stacked well placements, the Preese Hall wellbore is classified into strata according to their mineralogical- and sonic-determined geomechanical properties. The input logs (BI and P_b parameters) are normalised, and then inserted into a clustering algorithm. A k-means algorithm (Pedregosa et al., 2011) is used which seeks to minimize the "inertia" parameter (sum of squared distances of samples to their nearest cluster centre). The user is required to input the number of clusters to be defined, k. To determine the optimal number to be used, silhouette analysis was carried out (Pedregosa et al., 2011). This method calculates how far a sample is from neighbouring clusters, expressed as the silhouette coefficient. In analysing the plots, the user is seeking to pick a k value where most samples fall above the average silhouette score, and also where each cluster has approximately the same number of samples (shown as the thickness of the silhouette plot). In this analysis, a k value of 4 was chosen (Figure 5).

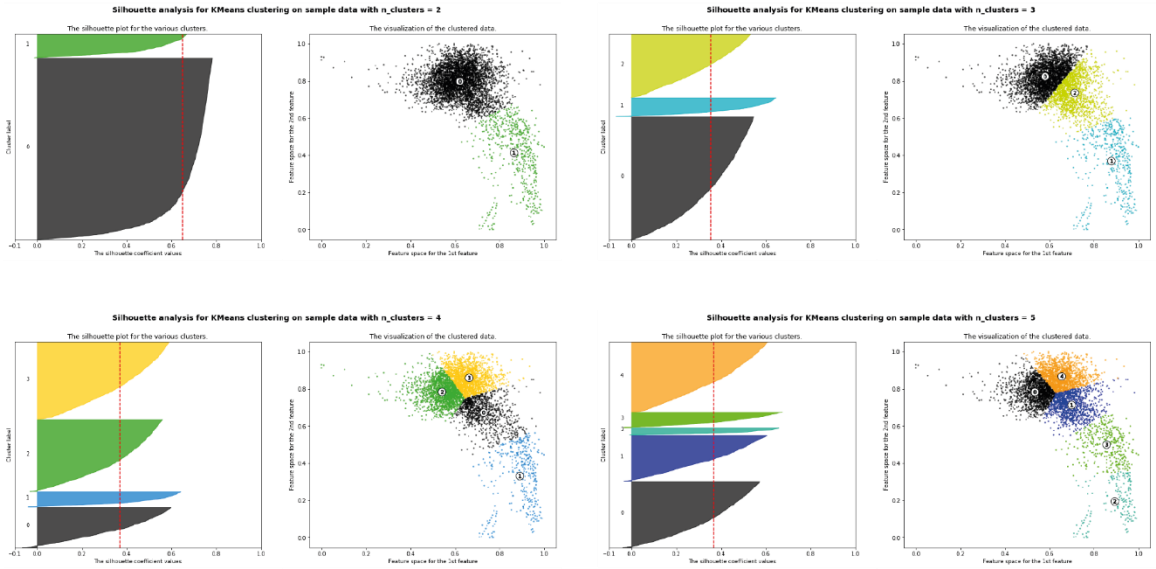

Figure 5 Silhouette analysis plots for cluster analysis. These plots help define the number of clusters to be input to the k-means algorithm. The silhouette score measures the distance of each sample from neighboring clusters. A favourable result is considered when all values plot greater than the average silhouette score (dotted red line) and where each cluster size approximately equal

Results

A nonlinear negative correlation exists between BI and P_b, although there is considerable scatter (Figure 6). Two trends could be interpreted: one showing a small decrease in BI for each relatively large increase in P_b at its low end (observed in clusters 0, 1 and 2), and another showing a large increase in BI for each relatively small increase in P_b at its high end (observed in cluster 3).

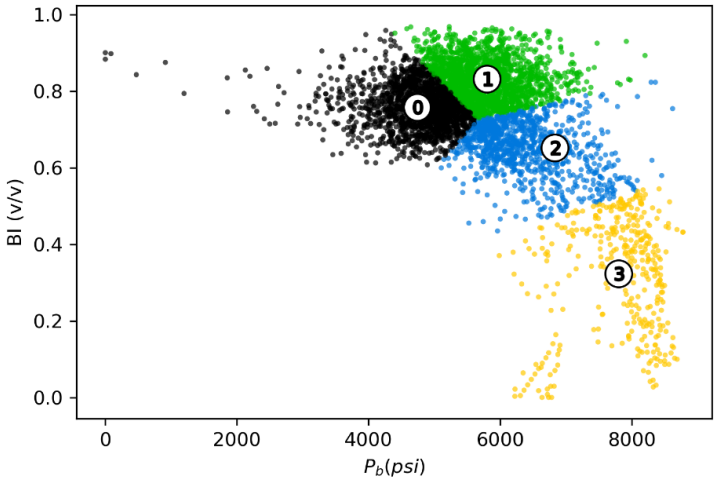

Figure 6: P_b versus BI scatter plot with datapoints coloured and labelled by clustering output.

A zone in which a stimulated hydraulic fracture should propagate with ease will have a high BI and low P_b. Therefore, the most optimal zone in this model is cluster 0 (black). Cluster 1 (green) also shows favourable properties but with around 1000 psi greater P_b. Cluster 2 (blue) has a similar P_b to cluster 1 and therefore they may have similar fraccability. However, cluster 2 has lower BI than cluster 0 or 1 which suggests it behaves in a more ductile manner, making it harder to keep fractures open using proppants. Although clusters 2 and 3 fall into the similar intervals of P_b, the former has much higher BI than the latter, making the latter being the least favourable class.

Figure 7 illustrates the vertical distribution of these geomechanical zones in Preese Hall. The main cluster 0 zones are found at 2000m, 2040m, 2165m, 2230m and 2336m; all within the Upper Bowland Shale. Thinner cluster 0 zones are seen in the Lower Bowland shale (e.g. 2578m), but most of this section is classified as cluster 1, indicating a greater P_b. The interval at 2336m is around 80m thick with only thin cluster 2 zones and forms the most prospective zone identified in this model. The cluster 4 zones appear to correlate with the clay-rich sections of the shale and are prevalent in the Lower Bowland Shale.

Discussion

Comparison with published work

Following an induced seismic event near the Preese Hall wellbore (Clarke et al., 2014b), several technical reports were commissioned to study its behaviour, which were summarized in (De Pater and Baisch, 2011). A geomechanical model was constructed as part of these studies and later expanded on by Clarke et al (2018). As presented in the methodology section, this work uses calibration data from these works but sought to calculate geomechanical parameters independently, in order to build a unique classification. However, geomechanical curves from Clarke et al (2018) were digitized in order to quality-check the models developed in this work and are presented in Figure 8 for visual comparison. While this work modelled lower pore pressure and σ_v values, the magnitudes of σ_h and σ_H are comparable. The difference in pore pressure requires further study, but given the difference in methodology used, these were considered adequate results. The increase in modelled quartz fraction observed in the Upper Bowland

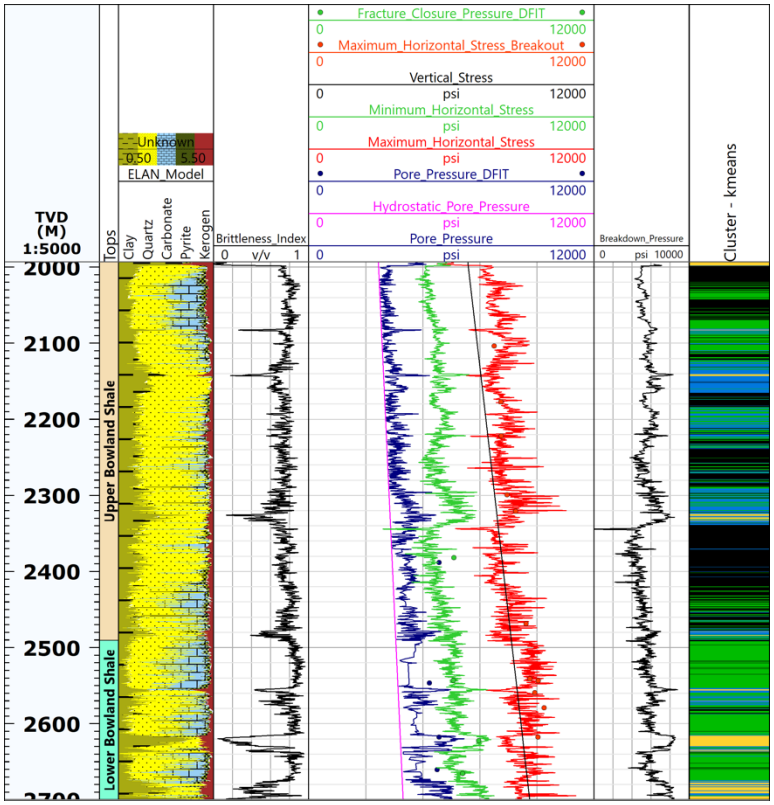

Figure 7: Plot of final outputs including mineralogy log, Brittleness Index, in situ stresses, breakdown pressure and corresponding cluster zone. The datapoints refer to calibration data from Clarke et al (2018).

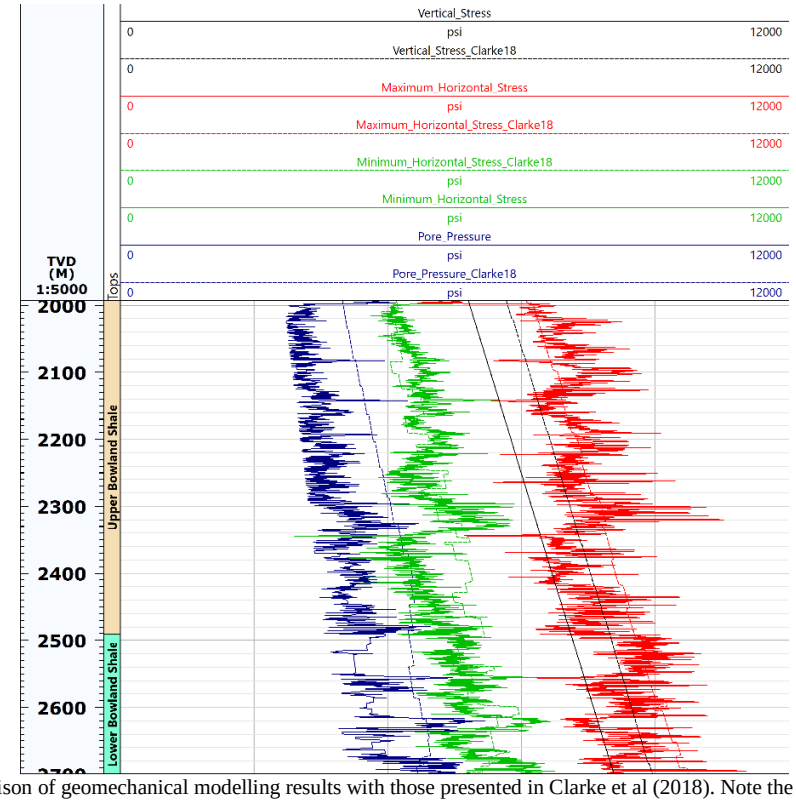

Figure 8: A comparison of geomechanical modelling results with those presented in Clarke et al (2018). Note the comparison data is digitized from the published paper and should only be used to assess the general trend.

Shale agrees with the theory that Namurian deposition in the region was being increasingly influenced by

large river systems and deltas ((Aitkenhead et al., 1992; Brandon et al., 1998; Kirby et al., 2000)). These ultimately culminated in the deposition of sand-rich sequences within the overlying Millstone Grit. This event is important in delineating the best geomechanical zone for fracture propagation.

Well placement

Six regions are identified where cluster 0 zones dominate (Table 1, Figure 9). Two of these (zones 4 and 5) are highlighted as potential landing sites for a lateral well. An assumption is introduced that fracture propagation is unlikely to extend further than 100m based on Davies et al (2012)'s study on US shale-gas microseismicity. While prospective zone 1 appears to have good geomechanical properties over a thick interval, it is only tentatively highlighted as it lies in close proximity to overlying Pendle Grit sandstones. Prospective zones 2, 3 and 6 are also identified, but the best geomechanical properties are restricted to thin intervals (~10-20m).

Clay-rich zones may act as fracture barriers, but further work is required to assess their impact. Analysis of natural fractures has been neglected in this study, initial analysis of FMI logs indicates that where present, they do not cross into clay-rich zones. Furthermore, the naturally fractured carbonates/siltstones, which may be below log resolution (Figure 3) will affect the geomechanical properties of the formation themselves. When combined with non-fractured ductile shale, they may provide a complex path for fracture propagation at resolutions smaller than presented in this modelling work.

Table 1 List of prospective zones, determined as regions where cluster 0 is the dominant cluster over a 10m interval. Zones 4 and 5 are identified as the optimal locations for landing horizontal wells.

Prospective zone	Interval	Thickness	Comments
1	1998-2069m	71m	Close to top of section and Pendle Grit
2	2111-2122m	11m	Thin
3	2165-2185m	20m	Thin
4	2226-2291m	65m	Good target
5	2336-2478m	142m	Good target
6	2576-2587m	11m	Thin

Conclusions

A geomechanical model, incorporating in situ stresses and mineralogy-derived brittleness index, was developed for the Bowland Shale section of the Preese Hall borehole. Using this model, two zones can be identified as suitable candidates for placing lateral wells. The first is located at the base of the Upper Bowland Shale and is where the best geomechanical properties are found. The second is within the Lower Bowland Shale, but may be limited by the presence of thick, clay-rich units. While this forms an important screening strategy, the impact of sub-wireline-scale heterogeneity visible using FMI. Such a strategy is important due to the structural complexity and geological heterogeneity within the Bowland Basin, owed to its tectonic complexity. Further investigation will be carried out in analyzing the elastic properties of sub-wireline-scale fractured units as these are not represented in this model. Furthermore,

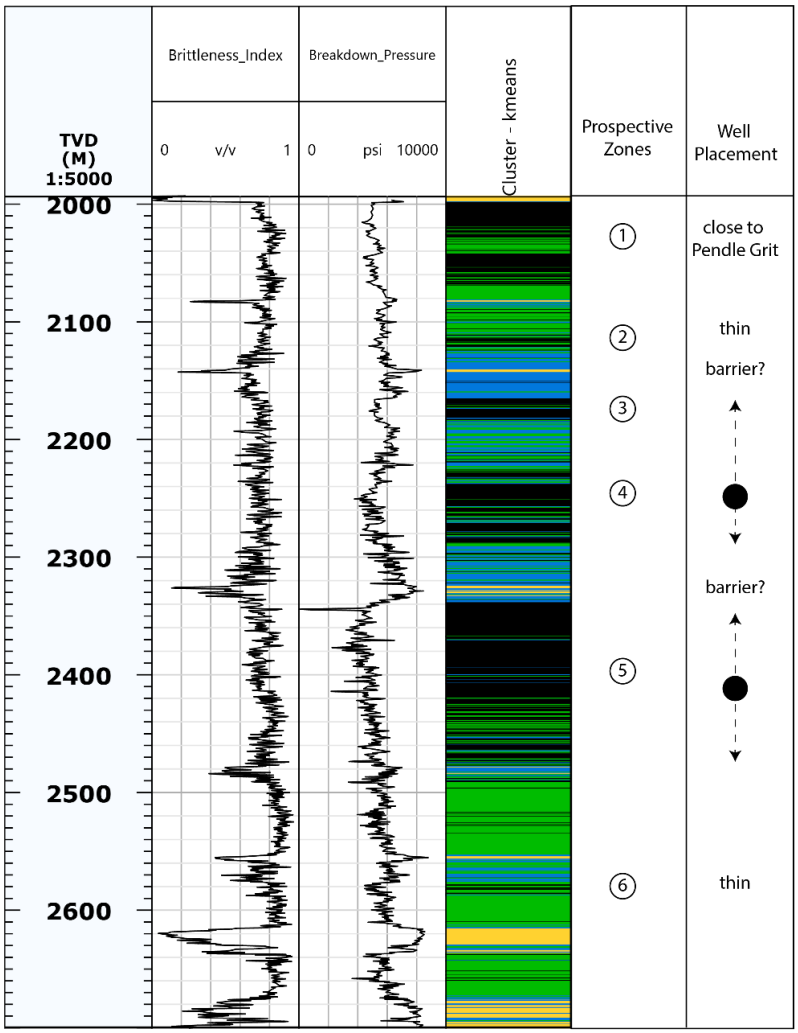

Figure 9: Suggested well placements based on the cluster analysis of Brittleness Index and Breakdown Pressure parameters. Black dots represent proposed landing sites, dashed lines represent approximate heights of fracture propagation based on Davies et al (2012).

wireline logs should be analysed at the newest sites of shale-gas exploration (Preston New Road 1, 2) to determine if the geomechanical zones identified here extend to these sites.

Acknowledgements

The work contained herein was conducted during a PhD study undertaken as part of the Natural Environment Research Council (NERC) Centre for Doctoral Training (CDT) in Oil & Gas (grant number NEM00578X/1). It is jointly funded by James Watt Scholarship Scheme of Heriot-Watt University and British University Funding Initiative (BUFI) of the British Geological Survey (BGS). The authors would also like to thank Schlumberger for the provision of Techlog and Petrel software under academic license to Heriot-Watt University, and the UK Onshore Geophysical Library (UKOGL)'s for access to their Beneath Britain Hub through which the seismic data was obtained. David Griffiths is also thanked for his discussions, encouragement and advice throughout.

References

Aitkenhead, N., Bridge, D.M., Riley, N.J., Kimbell, S.F., 1992. Geology of the country around Garstang. Memoir for the 1:50 000 geological sheet 67. British Geological Survey, HMSO, London.

Arthurton, R.S., 1984. The Ribblesdale fold belt, NW England—a Dinantian-early Namurian dextral shear zone. Geological Society, London, Special Publications 14, 131–138. https://doi.org/10.1144/GSL.SP.1984.014.01.13

Bott, M.H.P., 1967. Geophysical investigations of the northern Northern Pennine basement rocks. Proceedings of the Yorkshire Geological Society 36, 139–168. https://doi.org/10.1144/pygs.36.2.139

Brandon, A., Aitkenhead, N., Crofts, R.G., Ellison, R.A., Evans, D.J., Riley, N.J., 1998. Geology of the country around Lancaster. Memoir for the 1:50 000 Geological Sheet 59 (England and Wales). British Geological Survey, HMSO, London.

Clarke, H., Bustin, M., Turner, P., 2014a. Unlocking the Resource Potential of the Bowland Basin, NW England. Society of Petroleum Engineers. https://doi.org/10.2118/167776-MS

Clarke, H., Eisner, L., Styles, P., Turner, P., 2014b. Felt seismicity associated with shale gas hydraulic fracturing: The first documented example in Europe: Hydraulic fracturing, induced seismicity. Geophysical Research Letters 41, 8308–8314. https://doi.org/10.1002/2014GL062047

Clarke, H., Turner, P., Bustin, R.M., Riley, N., Besly, B., 2018. Shale gas resources of the Bowland Basin, NW England: a holistic study. Petroleum Geoscience. https://doi.org/10.1144/petgeo2017-066

Corfield, S.M., Gawthorpe, R.L., Gage, M., Fraser, A.J., Besly, B.M., 1996. Inversion tectonics of the Variscan foreland of the British Isles. Journal of the Geological Society 153, 17–32. https://doi.org/10.1144/gsjgs.153.1.0017

Cuadrilla Resources, 2019. Cuadrilla shale gas initial flow test results [WWW Document]. Cuadrilla. URL https://cuadrillaresources.com/media-resources/press-releases/cuadrilla-shale-gas-initial-flow-test-results/ (accessed 4.24.19).

Davies, R.J., Mathias, S.A., Moss, J., Hustoft, S., Newport, L., 2012. Hydraulic fractures: How far can they go? Marine and Petroleum Geology 37, 1–6. https://doi.org/10.1016/j.marpetgeo.2012.04.001

De Pater, C.J., Baisch, S., 2011. Geomechanical study of Bowland Shale seismicity. Synthesis report 57.

Earp, J.R., Magraw, D., Poole, E.G., Land, D.H., Whiteman, A.J., Calver, M.A., Ramsbottom, W.H.C., Sabine, P.A., 1961. Geology of the country around Clitheroe and Nelson : One Inch Geological Sheet 68, New Series, Geological Survey of Great Britain. England and Wales.

Eaton, B.., 1975. The equation for geopressure prediction from well logs. Presented at the Fall Meeting of the Society of Petroleum Engineers of AIME, Dallas, Texas. https://doi.org/10.2118/5544-MS

Economides, M.J., Martin, T. (Eds.), 2007. Modern fracturing - enhancing natural gas production. ET Publishing, Houston, Tex.

Economides, M.J., Nolte, K.G., 2000. Reservoir Stimulation, 3rd ed. Wiley.

Fraser, A.J., Gawthorpe, R.L., 2003. An Atlas of Carboniferous Basin Evolution in Northern England, Geological Society Memoir 28.

Hubbert, M.K., Willis, D.G., 1957. Mechanics of Hydraulic Fracturing. Petroleum Transactions, AIME 210, 16.

Jaeger, J.C., Cook, N.G.W., Zimmerman, R.W., 2007. Fundamentals of rock mechanics, 4th ed. Blackwell Pub, Malden, MA.

Jarvie, D.M., Hill, R.J., Ruble, T.E., Pollastro, R.M., 2007. Unconventional shale-gas systems: The Mississippian Barnett Shale of north-central Texas as one model for thermogenic shale-gas assessment. AAPG Bulletin 91, 475–499. https://doi.org/10.1306/12190606068

Jin, X., Shah, S.N., Roegiers, J.-C., Zhang, B., 2014. Fracability Evaluation in Shale Reservoirs - An Integrated Petrophysics and Geomechanics Approach, in: SPE Hydraulic Fracturing Technology Conference. Presented at the SPE Hydraulic Fracturing Technology Conference, Society of Petroleum Engineers, The Woodlands, Texas, USA. https://doi.org/10.2118/168589-MS

Johnson, G.A.L., 1967. Basement control of Carboniferous sedimentation in Northern England. Proceedings of the Yorkshire Geological Society 36, 175–194. https://doi.org/10.1144/pygs.36.2.175

Kirby, G.A., Baily, H.E., Chadwick, R.A., Evans, D.J., Holliday, S., Hulbert, D.W., Pharoah, T.C., Smith, N.J.P., Aitkenhead, N., Birch, B., 2000. Structure and evolution of the Craven Basin and adjacent areas, Subsurface geology memoirs. British Geological Survey.

Pedregosa, F., Varoquaux, G., Gramfort, A., Michel, V., Thirion, B., Grisel, O., Blondel, M., Prettenhofer, P., Weiss, R., Dubourg, V., Vanderplas, J., Passos, A., Cournapeau, D., 2011. Scikit-learn: Machine Learning in Python. Journal of Machine Learning Research 12, 6.

Peng, S., Zhang, J., 2007. Engineering geology for underground rocks. Springer, Berlin ; New York.

Rickman, R., Mullen, M.J., Petre, J.E., Grieser, W.V., Kundert, D., 2008. A Practical Use of Shale Petrophysics for Stimulation Design Optimization: All Shale Plays Are Not Clones of the Barnett Shale. Society of Petroleum Engineers. https://doi.org/10.2118/115258-MS

Waters, C.N., Waters, R.A., Barclay, W.J., Davies, J.R., 2009. A lithostratigraphical framework for the Carboniferous successions of southern Great Britain (onshore) (No. RR/09/01), British Geological Survey Research Report.

Zhang, C., Dong, D., Wang, Y., Guan, Q., 2017. Brittleness evaluation of the Upper Ordovician Wufeng–Lower Silurian Longmaxi shale in Southern Sichuan Basin, China. Energy Exploration & Exploitation 35, 430–443. https://doi.org/10.1177/0144598716687929

Zhang, D., Ranjith, P.G., Perera, M.S.A., 2016. The brittleness indices used in rock mechanics and their application in shale hydraulic fracturing: A review. Journal of Petroleum Science and Engineering 143, 158–170. https://doi.org/10.1016/j.petrol.2016.02.011

Zhang, J., 2011. Pore pressure prediction from well logs: Methods, modifications, and new approaches. Earth-Science Reviews 108, 50–63. https://doi.org/10.1016/j.earscirev.2011.06.001

Zoback, M.D., 2007. Reservoir geomechanics. Cambridge University Press, Cambridge.